PHYSICAL REVIEW B **68**, 140101(R) (2003)

X-ray image reconstruction from a diffraction pattern alone

S. Marchesini,[1,*] H. He,[2] H. N. Chapman,[1] S. P. Hau-Riege,[1] A. Noy,[1] M. R. Howells,[2] U. Weierstall,[3] and J. C. H. Spence[3]
[1]*Lawrence Livermore National Laboratory, 7000 East Avenue, Livermore, California 94550-9234, USA*
[2]*Lawrence Berkeley National Laboratory, 1 Cyclotron Road, Berkeley, California 94720, USA*
[3]*Arizona State University, Department of Physics, Tempe, Arizona 85287-1504, USA*
(Received 26 June 2003; published 28 October 2003)

A solution to the inversion problem of scattering would offer aberration-free diffraction-limited three-dimensional images without the resolution and depth-of-field limitations of lens-based tomographic systems. Powerful algorithms are increasingly being used to act as lenses to form such images. Current image reconstruction methods, however, require the knowledge of the shape of the object and the low spatial frequencies unavoidably lost in experiments. Diffractive imaging has thus previously been used to increase the resolution of images obtained by other means. Here we experimentally demonstrate an inversion method, which reconstructs the image of the object without the need for any such prior knowledge.

DOI: 10.1103/PhysRevB.68.140101 PACS number(s): 61.10.Nz, 42.30.Rx, 42.30.Wb, 68.37.Yz

The inversion problem of coherent scattering—the reconstruction of a single-scattering potential from measurements of scattered intensity in the far field—has occupied physicists for over a century, and arises in fields as varied as optics, astronomy, x-ray crystallography, medical tomographic imaging, holography, electron microscopy, and particle scattering. A solution to this problem would offer diffraction-limited images of nonperiodic objects without the use or need for a lens. The possibility of solving the x-ray phase problem for an isolated object was first suggested by Sayre[1] in 1952, who pointed out that Bragg diffraction in crystals undersamples the diffracted intensities.[2–4] The Bragg limitation on sampling is lifted for nonperiodic objects, which allow finer sampling of the diffraction pattern. An iterative phase-retrieval method, capable of phasing adequately sampled diffracted intensity first appeared in 1972[5]), followed by important theoretical advances due to Fiddy, Bates, and others—see Ref. 6 for a review. The iterative algorithm was greatly improved through the introduction of feedback and compact support (the support is the boundary of the object) by Fienup around 1982 with the hybrid input-output (HIO) algorithm,[7] which allowed inversions of optical data.[8,9] A significant breakthrough occurred in 1999 with the reconstruction by Miao and co-workers of a two-dimensional nonperiodic x-ray image at 0.075-μm resolution from diffraction data and a low-resolution image of the object.[10] Subsequent work has produced nanocrystal images at submicron resolution using hard x rays,[11] and striking tomographic images at higher resolution,[12] using zone-plate x-ray images to provide the low-resolution data. Images have also been obtained by inversion of experimental coherent electron-diffraction patterns,[13] and further laser-light images.[14] In one proposed application, atomic-resolution images might be obtained by the inversion of x-ray pulses diffracted from single molecules.[15] More generally, the possibility of using particles with low radiation damage has stimulated a burst of recent activity.[16]

The iterative algorithms, such as the HIO algorithm, iterate between real and reciprocal space, applying various *a priori* constraints in each domain. In diffraction space, the modulus squared of the diffracted wave field is set equal to the measured diffraction intensities, whereas in real space the transmission function of the object is set to zero outside the known boundary of the object (the support). Other constraints, which have been used, include the known sign of the scattering function and the various symmetries of the scatterer. These constraints may be classified as convex or nonconvex, and the theory of Bregman projections can be used to understand their convergence properties.[6] In theory, and confirmed by simulation, the support mask need not trace the exact boundary of the object (loose support), and zero (transparent) regions of the object inside the support may converge to their correct value without being forced by the mask. However, in practice, a less than perfect estimate of the support often prevents the reconstruction of the correct image[17])—see also below. Efforts to obtain the support function of the object from the support of the experimentally accessible autocorrelation function have been proposed for special classes of objects using elegant geometrical methods[18]). Methods for inverting Patterson maps to charge densities for crystals and nonperiodic objects are reviewed by Buerger[19]). Up until now, no images have been reconstructed from experimental x-ray-diffraction patterns of arbitrary objects without a lower-resolution image provided by an optic.

In this paper we eliminate the need for this secondary image and demonstrate ultrahigh resolution imaging without the need for a lens. The object support function is determined together with the object itself, without additional spatial information. The procedure builds on the HIO algorithm, in which constraints are iteratively applied in real and reciprocal space, and a feedback parameter is used in real space to damp the application of the support constraint. Feedback allows this algorithm to emerge from local minima of the invariant error metric and thus avoid stagnation. The uniqueness of solutions found by this method has been studied in detail[20] (rare ambiguous solutions have been found in two dimensions in cases where the spectrum is factorable). Our innovation is the simple but powerful use of the current estimate of the object to determine the support constraint. The first estimate of the support is the support of the autocorrelation function.[19] Although this estimate is far from accurate,

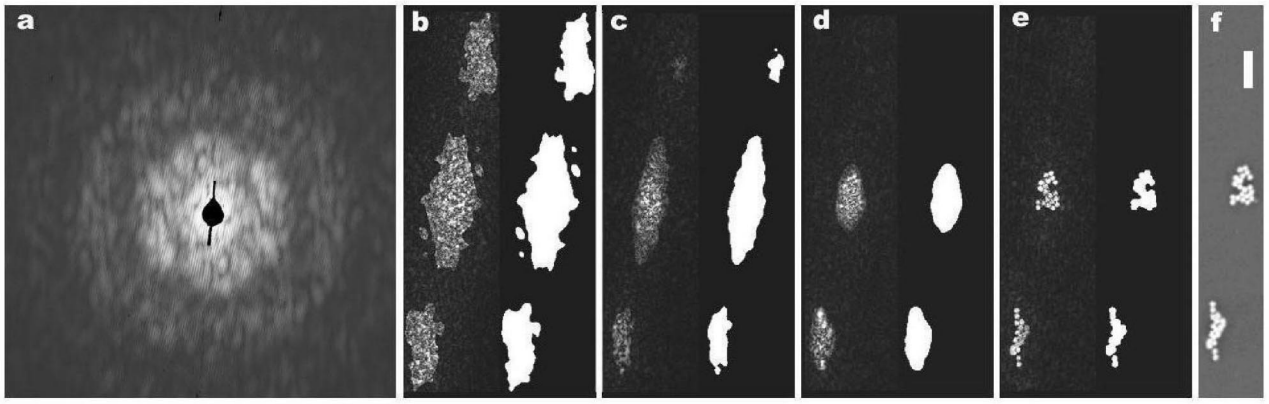

FIG. 1. Image reconstruction from an experimental x-ray-diffraction pattern. (a) X-ray diffraction pattern of a sample of 50-nm colloidal gold particles, recorded at a wavelength of 2 nm. (b–e) shows a sequence of images produced by the algorithm as it converges. Number of iterations: 1 (b), 20 (c), 100 (d), and 1000 (e). The reconstruction progresses from the autocorrelation function in (b) to an image in (e) with a steady improvement of the support boundary (shown at the bottom of each frame). For comparison, a scanning electron micrograph of the object is shown in (f). The scale bar length is 300 nm and the resolution of our reconstructed image is about 20 nm.

it is continually updated by thresholding the intensity of a blurred version of the current estimate of the object under reconstruction. Thresholding traces the boundary of the object at a given intensity contour. The blurring acts to smooth out noise and provides a form of regularization. In turn, through the normal behavior of the HIO algorithm, the improved support constraint gives rise to yet a better estimate of the object. We find that this method is very stable, and converges to the correct support and object for both simulated and experimental x-ray-diffraction data. The algorithm also successfully reconstructs complex objects (those that cause large variations in the phase of the exit wave field in two dimensions), which hitherto have been experimentally difficult to reconstruct.[8,9,13] This opens up the possibility of image reconstruction from microdiffraction patterns, where the illumination is tightly focused on the object.

Details of the algorithm are as follows. We start from the autocorrelation function of the object. This real-space map, obtained by Fourier transforming the diffraction pattern, displays all ''interatomic'' vectors, with peaks for all vectors between isolated objects, shifted to a common origin. It contains many more peaks than the object, and, even for an acentric object, possesses a center of inversion symmetry. Since the object must fit within the autocorrelation function, our first estimate of the support is a mask obtained from this function using a contour at the 4% intensity level. Both the correct object density and its centrosymmetric inversion fit within this initially centric mask, however, inversion symmetry is progressively lost as the algorithm converges. We then apply the HIO algorithm with feedback parameter $\beta = 0.9$ and the real-space support given by the calculated mask. We obtain the part of the diffraction pattern covered by a central beam stop from the transform of the current estimate of the object. Low-frequency components are treated as free parameters. Every 20 iterations we convolve the reconstructed image (the absolute value of the reconstructed wave field) with a Gaussian of width σ (full width at half maximum of 2.3548σ) to find the new support mask. The mask is then obtained by applying a threshold at 20% of its maximum. The width σ is set to 3 pixels in the first iteration, and reduced by 1% every 20 iterations down to a minimum of 1.5 pixels. Similarities of the original Gerchberg-Saxton algorithm with the ''solvent flattening'' method suggest that this method could be extended to crystallography.

We have tested the method using two-dimensional experimental data as well as two- and three-dimensional sets of simulated data. The experimental soft x-ray transmission diffraction pattern from two clusters of gold balls of 50 ± 5 nm diameter deposited on a silicon nitride window was recorded at the Advanced Light Source at the Lawrence Berkeley Laboratory, using soft x rays with a wavelength of 2.1 nm.[21,22] In Fig. 1 we present the experimental diffraction pattern and the sequence of images produced by the algorithm as it converges. As shown in the first step, the algorithm starts with a support mask with perfect inversion symmetry. After a few iterations the symmetry is broken. First, one of the three regions of the mask disappears, and then the support envelope shrinks progressively around the gold ball objects. Finally, a stable solution showing excellent agreement with a scanning electron microscope image of the same object is obtained. The solution also agrees well with a previous reconstruction by a different method.[21] Note that we would not expect a perfect match between the electron and x ray images, since image formation processes are different for electrons and x-rays. Repeated computational trials have all shown the same degree of convergence to the correct image or its centrosymmetric inversion. Although after a few hundred iterations the algorithm always converged to the correct image (independent of the initial random choice of phases), as iterations were carried further both the support and the image show arbitrary displacements due to the translational invariance of the solution.

To further assess the validity of the algorithm we have tested it on several sets of simulated diffraction patterns from gold spheres and gray-scale images. The simulations all include noise and the loss of data due to a central beam stop. They show that the algorithm is successful to the same degree as the standard HIO algorithm with tight support. As

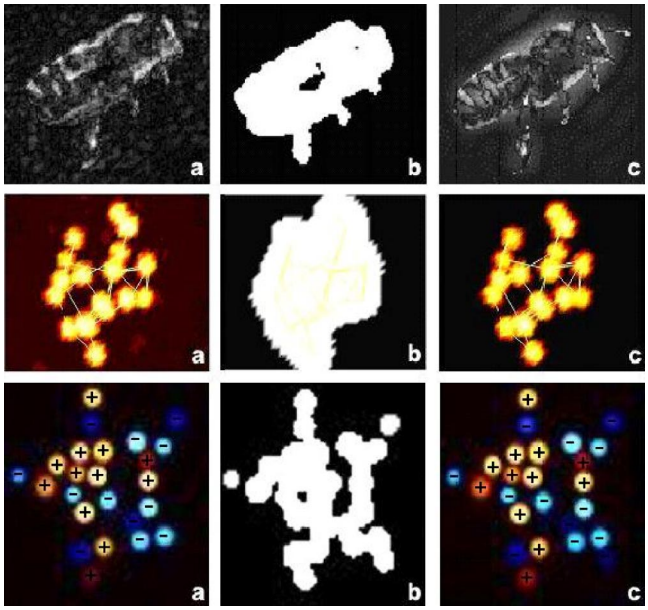

FIG. 2. (Color online) Image reconstructions from simulated diffraction patterns of a gray-scale image (top row), a 3D cluster of gold balls (center row) and a complex object illuminated with a complex focused probe (bottom row). In each row (a) is the recovered object, (b) the recovered support, and (c) the original image. The gray-scale image demonstrates that the algorithm does not depend on any ''atomicity'' constraint provided by the gold balls. For the complex object the real part is shown, blue is negative and red/yellow is positive.

examples, we include in Fig. 2 the reconstructions of a gray-scale image, a three-dimensional (3D) cluster of gold balls (ball diameter of 50 ± 5 nm), and a complex object illuminated by a focused beam. The gray-scale image demonstrates that the algorithm does not require any ''atomicity'' constraint provided by the gold balls. The particular 3D cluster was chosen to have a small number of balls for visualization purposes—the algorithm also works with a much larger number of balls. The third example is of particular interest since it is well known that the reconstruction of complex objects is much more difficult than real objects, but is possible using either disjoint, precisely known, or specially shaped supports.[17,14] Complex objects arise in optics and x-ray diffraction in two dimensions when large phase shifts occur within the eikonal approximation, or if that approximation fails, in the presence of spatially dependant absorption effects, and in the presence of multiple scattering. The question arises as to whether our method provides a sufficiently tight support, especially for objects fragmented into separated parts, to allow the inversion of complex objects. Figure 2 (bottom) shows the reconstruction of a cluster of gold balls where each ball is multiplied by a constant random phase shift between 0 and 2π. The cluster is singled out from neighboring ones by a focused beam. A perfect match between object and reconstruction is again observed if one takes into account the translation and constant phase invariance in the solution. The result is significant because it relaxes the requirement for plane-wave illumination. The generality of the technique is thus increased because now the

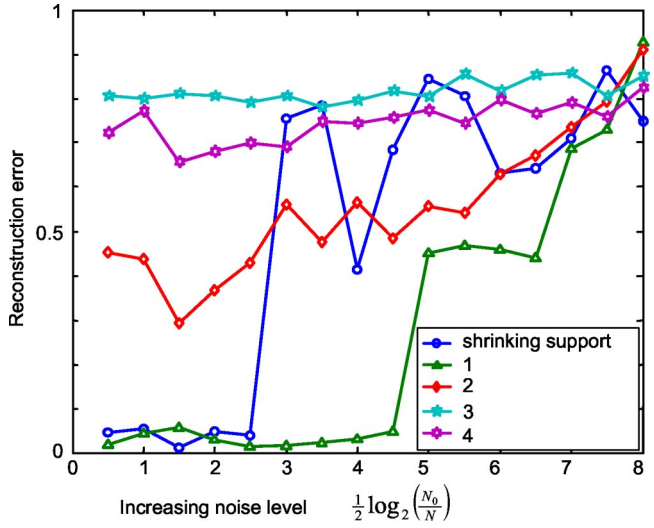

FIG. 3. (Color online) Reconstruction error of our algorithm and the HIO algorithm for a complex object as a function of Poisson noise in the diffraction image (N is the maximum number of photons per pixel, $N_0=2^{17}$). In the HIO algorithm increasingly looser supports (supports 1–4) are used: supports 1, 2 and 3 are obtained by thresholding the original image after convolving with a Gaussian of 0.5, 5, and 25 pixels width. Support 4 is obtained from the autocorrelation. The HIO algorithm with perfect support (support 1) works well even for high noise levels whereas it always fails with loose supports (supports 3 and 4). The algorithm (shrinking support) is superior to the HIO with limited knowledge of the support shape (supports 3 and 4). Our algorithm fails when the noise in real space becomes larger than the threshold used to update the support.

focused probe can be used to isolate objects in the image field.

We have compared the behavior of our algorithm to that of the HIO algorithm. The HIO algorithm requires the support *a priori*, and as is well known, the error in the reconstruction decreases as the support becomes tighter and closer to the actual boundary of the object. This is illustrated in Fig. 3, which shows plots of the reconstruction error, as a function of Poisson noise in the diffraction intensities, for the HIO algorithm with support masks of various degrees of accuracy. The masks for these cases were calculated by convolving the object by Gaussians of various widths (0.5, 5, and 25 pixels) and thresholding at 5% level from the maximum. This corresponds to knowing the shape of the object to a given resolution. It is seen that even for low noise, HIO can achieve a reasonable reconstruction only if the support mask is set to the boundary known at essentially the same resolution to which we are reconstructing the object. The reconstruction error for our algorithm (which does not require *a priori* knowledge of the support) is also plotted in Fig. 3. We expect that the noise level at which our algorithm fails to reconstruct occurs when the noise in real space becomes larger than the threshold used to update the support. At this noise level the estimate of the support will be influenced by the noise, and the algorithm will be unable to converge to the correct boundary. This suggests that the optimum threshold setting depends on the noise level in the data, and we will only be able to reconstruct those parts of the object where the

contrast is above the noise. As the support used in the HIO algorithm becomes looser, we observe our algorithm to be much superior, even in the presence of noise. This is because our algorithm always improves upon the support and so makes optimal use of the available information. The only prior knowledge needed is that the object possesses compact support (i.e., is isolated), so that oversampling diffraction conditions can be guaranteed experimentally, and that the contrast of the object is above the noise. By comparison with earlier methods,[16] no knowledge of the shape of the object is required. There are few adjustable parameters in our algorithm; namely, support resolution, support threshold, and feedback parameter. Additional constraints can be added to strengthen convergence, such as atomicity, positivity, and histogram matching.[23,24]

The combination of an apparatus to measure large-angle diffraction patterns with our method of data analysis forms a different type of diffraction-limited, aberration-free tomographic microscopy. The absence of inefficient optical elements makes more efficient use of damaging radiation, while the reconstruction from a three-dimensional diffraction dataset will avoid the current depth-of-field limitation of zone-plate-based tomography. The use of focused illumination will allow users to select either one- or two-part objects (which may be complex) from a field. The conditions of beam energy and monochromatization used in these preliminary experiments are far from optimum for diffractive imaging and can be greatly improved to reduce recording times by more than two orders of magnitude. We expect this microscopy to find many applications. Since dose scales inversely as the fourth power of resolution, existing measurements of damage against resolution can be used to show that statistically significant images of single cells should be obtainable by this method at 10 nm resolution in the 0.5–10 μm thickness range under cryomicroscopy conditions. Imaging by harder coherent x rays of inorganic nanostructures (such as mesoporous materials, aerosols, and catalysts) at perhaps 2-nm resolution can be expected. Atomic-resolution diffractive imaging by coherent electron nanodiffraction has now been demonstrated.[25] The imaging of dynamical systems, imaging with new radiations for which no lenses exist, and single molecule imaging with x-ray free-electron laser pulses remain to be explored.

We acknowledge stimulating discussions with Abraham Szöke. This work was performed under the auspices of the U.S. Department of Energy by the Lawrence Livermore National Laboratory under Contract No. W-7405-ENG-48 and the Director, Office of Energy Research, Office of Basics Energy Sciences, Materials Sciences Division of the U.S. Department of Energy, under Contract No. DE-AC03-76SF00098. S.M. acknowledges funding from the National Science Foundation. The Center for Biophotonics, an NSF Science and Technology Center, is managed by the University of California, Davis, under Contract No. PHY0120999.

*Author to whom correspondence should be addressed. Email address: smarchesini@llnl.gov

[1] D. Sayre, Acta Crystallogr. **5**, 843 (1952).

[2] Finer sampling of intensities is needed to satisfy Shannon's theorem (and hence solve the phase problem) since the autocorrelation function of the molecule acts as a band limit.

[3] D. Sayre, in *Image Processing and Coherence in Physics*, edited by M. Schlenker *et al.*, Springer Lecture Notes in Physics, Vol. 112 (Springer, Berlin, 1980), pp. 229–235.

[4] D. Sayre, H.N. Chapman, and J. Miao, Acta Crystallogr., Sect. A: Found. Crystallogr. **A54**, 232 (1998).

[5] R. Gerchberg and W. Saxton, Optik (Jena) **35**, 237 (1972).

[6] H. Stark, *Image Recovery: Theory and Applications* (Academic Press, New York, 1987).

[7] J.R. Fienup, Appl. Opt. **21**, 2758 (1982).

[8] J.N. Cederquist, J.R. Fienup, J.C. Marron, and R.G. Paxman, Opt. Lett. **13**, 619 (1988).

[9] Y. Kamura and S. Komatsu, Jpn. J. Appl. Phys., Part 1 **37**, 6018 (1998).

[10] J. Miao, C. Charalambous, J. Kirz, and D. Sayre, Nature (London) **400**, 342 (1999).

[11] I.K. Robinson, I.A. Vartanyants, G.J. Williams, M.A. Pfeifer, and J.A. Pitney, Phys. Rev. Lett. **87**, 195505 (2001).

[12] J. Miao, T. Ishikawa, B. Johnson, E.H. Anderson, B. Lai, K.O. Hodgson, Phys. Rev. Lett. **89**, 088303 (2002).

[13] U. Weierstall, Q. Chen, J.C.H. Spence, M.R. Howells, M. Isaacson, and R.R. Panepucci, Ultramicroscopy **90**, 171 (2002).

[14] J.C.H. Spence, U. Weierstall, and M.R. Howells, Philos. Trans. R. Soc. London **360**, 875 (2002).

[15] R. Neutze, R. Wouts, D. van der Spoel, E. Weckert, and J. Hajdu, Nature (London) **406**, 752 (2000).

[16] J.C.H. Spence, M.R. Howells, L.D. Marks, and J. Miao, Ultramicroscopy **90**, 1 (2001).

[17] J.R. Fienup, J. Opt. Soc. Am. A **4**, 118 (1987).

[18] J.R. Fienup, T.R. Crimmins, and W. Holsztynski, J. Opt. Soc. Am. **72**, 610 (1982).

[19] M.J. Buerger, *Vector Space, and its Application in Crystal-structure Investigation* (Wiley, New York, 1959).

[20] J.H. Seldin and J.R. Fienup, J. Opt. Soc. Am. A **7**, 412 (1990).

[21] H. He, S. Marchesini, M. Howells, U. Weierstall, G. Hembree, and J.C.H. Spence, Acta Crystallogr., Sect. A: Found. Crystallogr. **A59**, 143 (2003).

[22] H. He, S. Marchesini, M. Howells, U. Weierstall, H. Chapman, S. Hau-Riege, A. Noy, and J.C.H. Spence, Phys. Rev. B **67**, 174114 (2003).

[23] V. Elser, J. Opt. Soc. Am. A **20**, 40 (2003).

[24] Our adjustment of the support provides precisely what the histogram constraint needs: a continually updated estimate of the count of pixels of low object density.

[25] J.M. Zuo, I. Vartanyants, M. Gao, R. Zhang, and L.A. Nagahara, Science **300**, 1419 (2003).